

EXPERIENCE WITH CRASH SIMULATIONS USING AN IGA BODY IN WHITE

Frank Bauer¹, Tian Yugeng¹, Lukas Leidinger², Stefan Hartmann²

¹BMW AG
Knorrstraße 147, 80788 Munich, Germany

²DYNAmore GmbH, an ANSYS Company
Industriestr. 2, 70565 Stuttgart, Germany

1 Abstract

With the IGA (Isogeometric Analysis) technological approach [1], the transfer processes from CAD to CAE can be simplified in the future and false predictions due to discretization effects can be reduced. In recent years, IGA and the corresponding toolset has increasingly developed into a setup that comes close to industrial use [2].

In order to test the use of IGA in industrial environments, a body in white (BIW) that was previously modelled with a „classic“ FE approach was also modelled with IGA and installed in a so-called hybrid model in a full vehicle crash simulation. For this purpose, the CAD data used as the basis for the FE model creation was used to directly create IGA surfaces.

The aim of implementing a body in white using IGA was, on the one hand, to look at the processes in terms of usability, automation capability and implementation quality; and, on the other hand, to understand how hybrid crash simulations behave in terms of computing time and stability.

In order to see different design effects in crash simulations, a front crash and a side crash were carried out and compared with existing FE models.

The investigations show the entire process, from geometry conversion to full vehicle simulation and explain the findings in comparison with the FE model.

2 Motivation and Introduction

As stated in the abstract, the two main motivating factors for this study of an IGA BIW in crash simulations are (i) to evaluate the current IGA model generation and implementation processes, and (ii) to understand how hybrid IGA/FEA models behave and perform. Both aspects shall be studied within the scope of large-scale applications. This paper therefore focuses on the full vehicle level, although coupon and component level studies are also part of our IGA activities as Fig. 1 shows.

Since the IGA capabilities for both preprocessing and analysis are most advanced for shell structures, this paper is restricted to thin-walled shell components. Nevertheless, isogeometric (trimmed) solids have a large potential to improve the analysis of rather thick-walled components like cast components. More information about IGA solids can be found in the contribution by Hartmann et al. [3].

The chosen body in white is an attractive test bed because it mainly consists of thin-walled sheet metal components which can be modeled as shells and therefore also as IGA shells. Additionally, the FEA model generation for this BIW based on batch mesh processes is already highly automatized at BMW and therefore provides a good benchmark for IGA processes and tools.

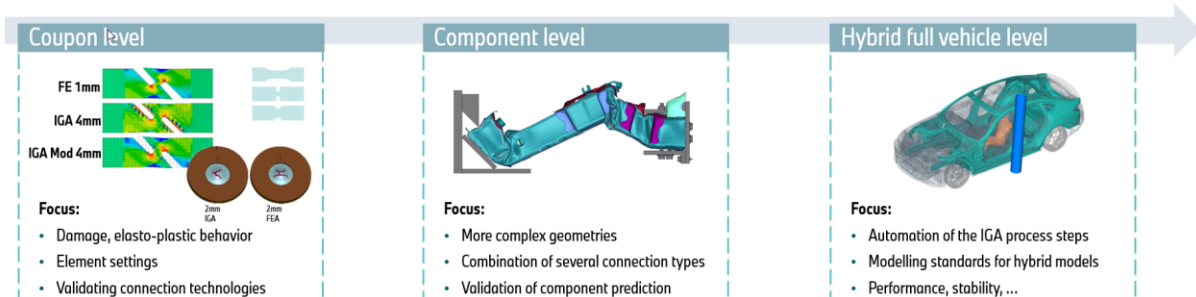


Fig.1: IGA activities at different levels of observation.

2.1 Potential of Faster Model Build Up for Sheet/Extrusion Parts with IGA Shells

In virtual vehicle development, one needs to distinguish between two scenarios. The first scenario is the initial simulation model build up from CAD data. This model build up process must ensure that various functional evaluations are based on the same geometric configuration. In the second scenario, functional evaluations of new geometric modifications are performed within various concept loops. In order to reduce response times to a minimum in both scenarios, it is important to implement the process of converting CAD data into a simulation model almost without manual effort and within the shortest possible time. Because IGA and CAD use the same geometric description based on NURBS (Non-Uniform Rational B-Splines) and a similar feature-based modeling technique, there is potential for a faster transition from CAD to simulation with future IGA-oriented processes, see Fig. 2.

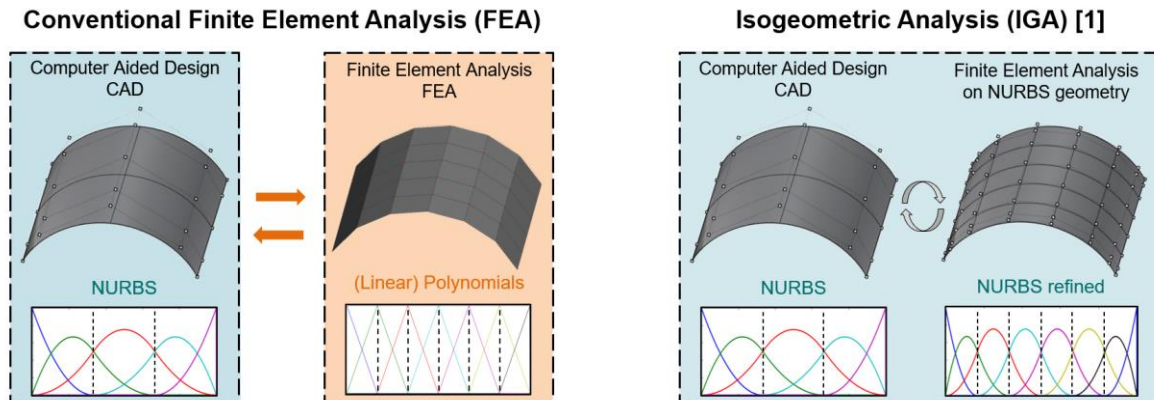


Fig.2: Transition from CAD to analysis for FEA (left) and IGA (right).

However, the similar model description used for IGA and CAD is not the only factor for optimizing today's processes. The main factors are:

1. Midsurface generation must run automatically or direct midsurface output from the CAD program must be made available.
2. Quick conversion of midsurfaces to IGA without previous meshing processes.
3. Computing time with IGA models must not be significantly higher than with current FE models, otherwise the advantage of fast model build up (scenario 1) is lost in the daily concept loops (scenario 2).

2.2 Potential of a Higher Prediction Quality

2.2.1 Faster mesh convergence

As demonstrated in several scientific studies [1,4] and other IGA-related papers of this conference [3,5,6], the higher-order and higher-continuity basis functions used for IGA can achieve more accurate results for a given element size compared to conventional (linear) finite elements, especially for smooth solutions. Or in other words, the same accuracy may be achieved with a larger element size, i.e. faster mesh convergence. The question that remains to be answered is how large the IGA element size can be chosen to capture small geometric features with reasonable accuracy. This is discussed in the following section.

2.2.2 Geometric Features, Time Step Size and Mass Scaling

Geometric features such as holes, beads or crimps are often used to trigger certain deformation patterns in passive safety concepts, to control vehicle acoustics or because of design space requirements. In order to reliably predict the effects of such (small) geometric features, very fine FE meshes are sometimes required in sensitive areas, which results in an undesired local increase in mass scaling. Although there are several options to address this in LS-Dyna for FEA (e.g. selective mass scaling), capturing this geometric features with larger mesh sizes is desirable. IGA with its spline-based elements offers a higher geometric accuracy for a given element size as shown in Fig. 3 and therefore has the potential to alleviate this issue.

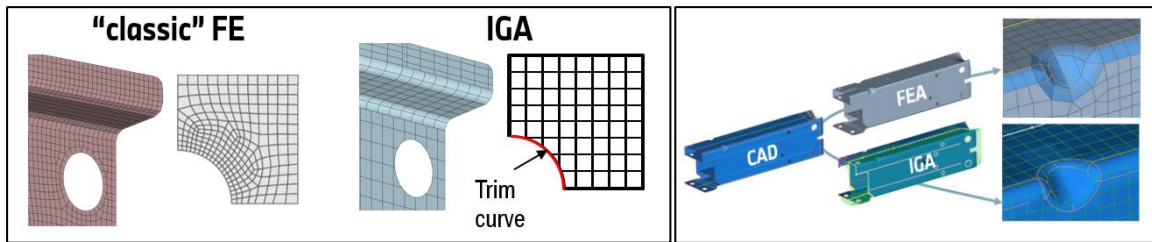


Fig.3: Geometric features modeled with FEA and IGA.

Furthermore, the larger stable explicit time step size of isogeometric elements compared to conventional linear finite elements [7] will lead to less mass scaling in crash simulations with a predefined time step size. The reason for the larger stable time step size for isogeometric elements lies in the higher order and, more importantly, higher continuity of NURBS basis functions. With the ANSA function “Extend” in IGA model creation (see Fig. 6), a larger time step can be achieved by cutting away the low-continuity elements at the patch boundary. This can be exploited with the improved time step estimate in LS-DYNA by setting IGADO=1 in `*CONTROL_TIMESTEP`. For biquadratic IGA elements, this means an increase in the time step of around 25%, for bi-cubic IGA elements by around 40% compared to linear finite elements [7]. Even if the time step in hybrid IGA/FEA vehicle crash simulations cannot be increased because it is still dominated by the FE components, the ratio between geometric accuracy and mass scaling is improved with IGA.

3 Hybrid IGA/FEA Model

3.1 Model Generation with ANSA

3.1.1 IGA Surface Generation

An existing classic FE BIW and its CAD data are used for the investigations. In a first step, the CAD data, in total 353 components, is converted into midsurfaces through a batch process. This step is the same as in traditional FE and necessary as a starting point for IGA surface creation (Fig. 4). Depending on the quality of the CAD data, the generation of the midsurfaces for sheet metal parts, can be fully automated.

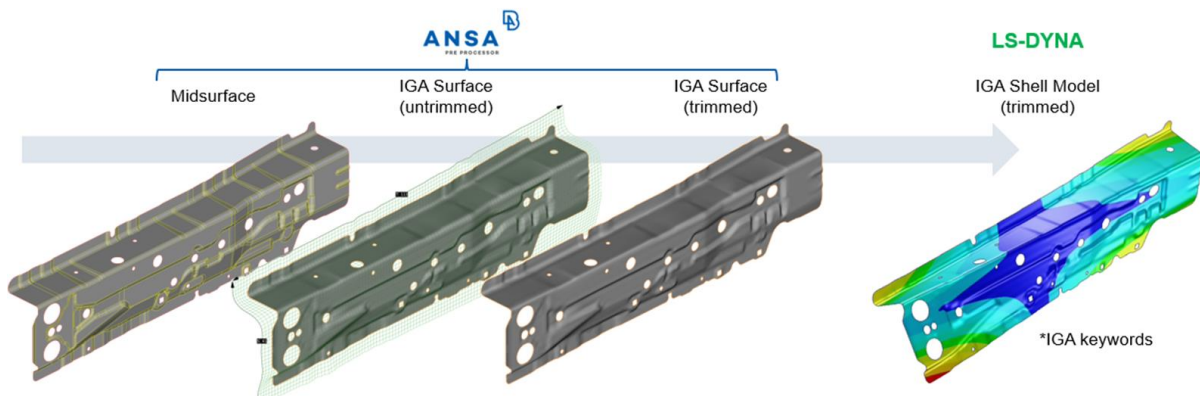


Fig.4: IGA surface generation: From the midsurface to an analysis-suitable IGA shell model.

Certain components were excluded in the IGA model generation, as shown in Fig 5.

1. Cast parts because they cannot be realized as shells.
2. Bushings and small connectors, because they are sometimes too thick to model as shells and were not relevant for this study.
3. Components with differing material properties in a single component (i.e. Tailor-welded or Tailor-rolled parts), because of lacking processes.

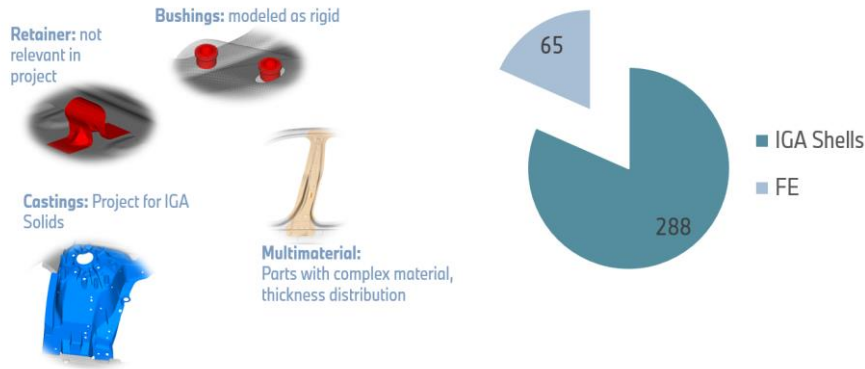


Fig.5: Components not modeled as IGA shells (left) and ratio between IGA and FE components (right).

In a second step, the 288 remaining parts are converted into analysis-suitable IGA surfaces (trimmed NURBS patches) using ANSA 23.1.x, see also Fig. 4. In order to accomplish this, ANSA uses a process that (if possible) generates a single IGA NURBS surface (patch) with a consistent element size and polynomial degree, out of multiple smaller CAD surfaces which are not suitable for analysis (very small surfaces or elements, and high polynomial degrees lead to poor performance). The IGA surfaces are generating with the settings shown in Fig. 6. Please note that *bi-quadratic* refers to the polynomial degree p . The *order* to be chosen in ANSA is defined as $p + 1$.

1. Bi-quadratic NURBS patches (Order=3)
2. Uniform element size (Min span = 4mm)
3. Joined surfaces (Join)
4. Enabled larger time step (Extend)

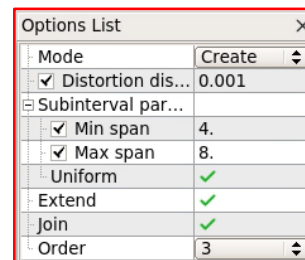


Fig.6: ANSA Settings for IGA surface creation.

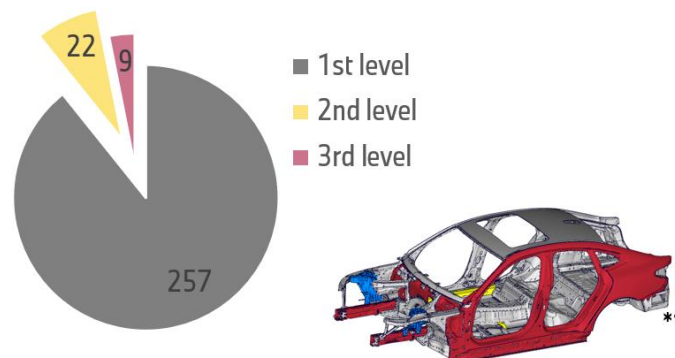
As observed during the creation of the IGA surfaces, complex or very large components like aluminum extrusion profiles or the side frame, could not be represented by single IGA surfaces (patches). As a result of this, extra manual effort is required to create those multi-patch parts.

In order to show the complete picture of how fully the IGA conversion process can be automated, the IGA components have been classified according to their complexity, as shown in Fig. 7.

1st level: One click, fully automated generation of IGA surfaces from CAD mid-surfaces.

2nd level: 1-3 small manual adjustments were required (obvious separation into multiple surfaces).

3rd level: High cost in time and effort, sometimes iteratively, with many manual adjustments (separating multiple surfaces)



*1 : Pictures don't show the IGA car model because of confidence reasons

Fig.7: Different complexity levels of components in the IGA surface creation process.

Two examples for components of level 3 complexity are the longitudinal beam (extrusion profile) and the side-frame (sheet metal part) depicted in Fig. 8. As can be seen, the longitudinal beam must be manually split into 22 IGA patches, the side-frame into 36.

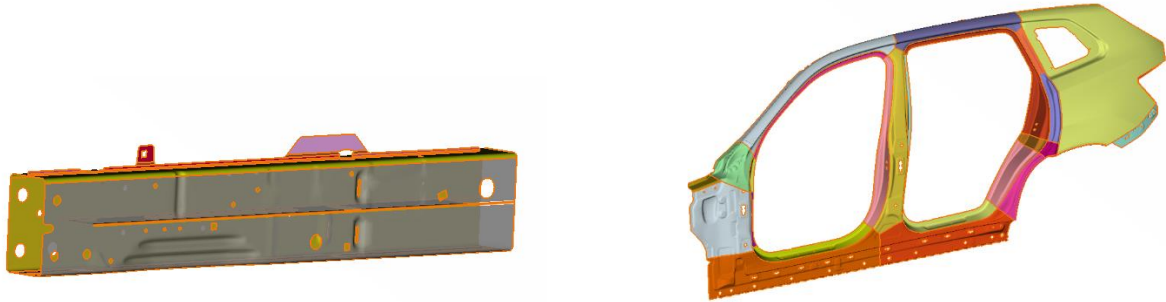


Fig.8: Example of a longitudinal beam and a side-frame modeled with 22 and 36 IGA patches, respectively (level 3 complexity).

3.1.2 Integration of IGA Components into an Existing FE Model

After the conversion, the 288 IGA parts need to be integrated into the existing FE BIW model. For this, the compatibility with the different joining technologies (screws, welds, adhesives) in the full vehicle model must be taken into consideration, see Fig. 9. The goal here was to see if the simple one-to-one substitution of the classical FE parts for IGA parts would work as a “plug and play” system, or if additional measures must be developed to have the IGA parts interface correctly with the rest of the hybrid model. The new LS-DYNA implementations and improvements required to achieve this are summarized in Section 3.2 below.

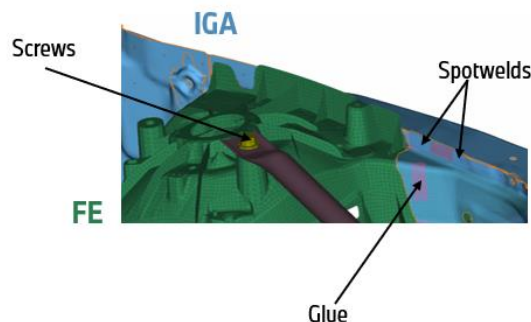


Fig.9: Integration of IGA parts require compatibility with existing connection technologies.

As a final step the BIW include with the 288 IGA components (which shall be referred to as the IGA BIW as it is mainly made of IGA parts), is integrated into preexisting full vehicle crash models, again with the focus of not having to change any contact, material, or coupling definitions in the full vehicle. It must be said here that the original FE parts all had mapping data describing their thicknesses and residual strains from the stamping process, these mappings were not carried over into the IGA BIW due to missing processes at that time. The mapping process for IGA can, however, now be achieved using the DYNAMore tool Envyo [8]. To keep the comparability the mapping information was also removed in the FEA BIW.

In summary, the integration of the IGA parts into the full vehicle model is comparable to the effort required for traditional FE models. No additional changes are required in the contact definitions, in the material definitions, the joining technology or the control settings. Only for node-based tied contacts and nodal rigid bodies it is necessary to project the original FE nodes onto the IGA surfaces using the LS-DYNA IGA keyword `*IGA_POINT_UVW`. This can be easily performed with a few clicks using the ANSA function `IGA > Points > Create`. It should be noted that similar steps are required for the substitution of

FE models. Also there, any free nodes of nodal rigid bodies have to be coupled to the new mesh using the ANSA function *branch* or *merge*.

3.2 Developments and Improvements in LS-DYNA for Hybrid IGA/FEA Modeling

The only notable change required for running the hybrid model was to use LS-DYNA R14, in order to use the latest ***IGA** keywords, and a different mass trim process to compensate for the lower mass scaling in the IGA components. The original FE simulation was also run again in R14 to ensure comparability.

To enable crash simulations of full hybrid IGA/FEA models and a simple 1:1 component exchange as described above, the following implementations and improvements were made in LS-DYNA (more details can be found in the contribution by Leidinger et al. [9]):

1. ***CONTACT_TIED_SHELL_EDGE_TO_SURFACE_CONSTRAINED_OFFSET** to constrain nodes with rotational DOFs (e.g. nodes of finite element shells) to IGA shells.
2. ***CONTACT_TIED_SHELL_EDGE_TO_SURFACE_BEAM_OFFSET**: Improved accuracy if used with nodes associated with parametric points (***IGA_POINT_UVW**) on IGA shells.
3. ***CONTACT_SPOTWELD** (**=*CONTACT_TIED_SHELL_EDGE_TO_SURFACE**) to constrain nodes of cohesive hexa solid elements to IGA shells.
4. Initialization of material history variables with ***INITIAL_STRAIN/STRESS_IGA_SHELL** and supporting the mapping in the DYNAmore tool Envyo [8].
5. Improved accuracy of trimming curves on curved isogeometric surfaces.
6. Edge contact exclusion along patch-coupling edges of isogeometric shells (***IGA_TIED_EDGE_TO_EDGE**).

With these implementations and improvements, stable crash simulations of both the hybrid front and side crash models with 288 IGA components could be performed. This is a significant progress compared to the two IGA components in the hybrid vehicle crash simulations presented at the German LS-DYNA Forum in 2022 [10] as shown in Fig. 10.

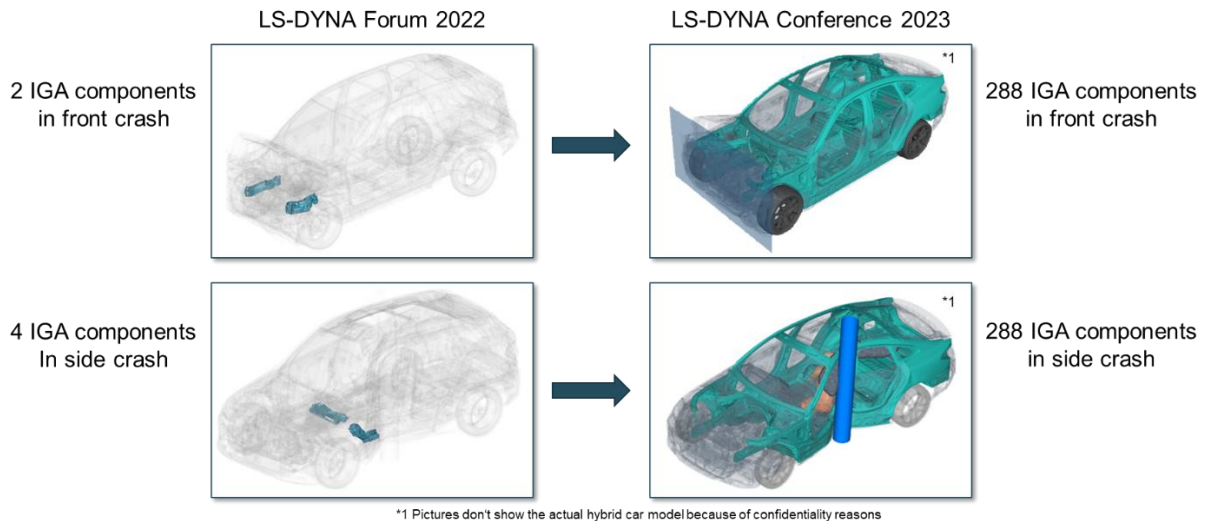


Fig.10: Progress in hybrid IGA/FEA vehicle modeling.

4 Hybrid Full Vehicle Crash Simulations

This section provides first results of hybrid full vehicle crash simulations with the IGA body in white presented above and comparisons with results from conventional FEA models. A meaningful comparison to hardware tests cannot be provided because processes to apply mapping data onto IGA shell models were not available at the time when the IGA model was generated.

4.1 Model Properties and Settings

The BIW integrated into the hybrid full vehicle model consists of 288 bi-quadratic IGA shell components with a shear-deformable Reissner-Mindlin element formulation (ELFORM=3), 2x2 in-plane integration points per element (reduced Gauss integration, IRL=0), five integration points in thickness direction and an average element size of 4mm (same as the reference FE model). For contact and visualization, an interpolation mesh with 2x2 linear elements per IGA element is used. This interpolation mesh consisting of null shells is automatically generated by LS-DYNA. The density of this mesh can be defined by the user via NISR and NISS in `*IGA_SHELL`. The coupling of NURBS patches for the multi-patch models (see level 2 and level 3 complexity in Section 3.1.2) is done via a weak penalty-based approach [7]. With these settings, robust and stable crash simulations of the hybrid vehicle model could be performed.

As a reference, a conventional FE vehicle model with linear Belytschko-Tsay elements (ELFORM=2) with one in-plane integration point, five integration points in thickness direction and an average shell element size of 4mm is used. As in the hybrid vehicle model, no mapping data is considered to allow comparability. For both models, mainly segment-based contact (SOFT=2) is used.

4.2 Load Case Descriptions and Motivation

4.2.1 Full Width Frontal Impact

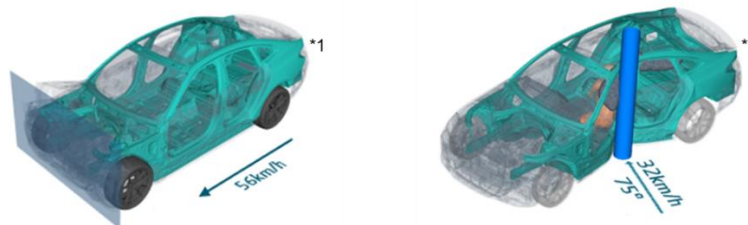
The first load case scenario investigated here, is a full width frontal impact of a full vehicle structure with 56km/h against a rigid wall barrier with 100% overlap as shown in Fig. 11 (left). The main motivation for this front crash scenario was to answer the following questions:

1. How do the IGA models of the main longitudinal beams (see Fig. 8) behave? These beams are part of the main load path in the front crash scenario and therefore crucial for the overall behavior. The corresponding IGA models are of complexity level 3 and consist of multiple trimmed patches which are coupled via a penalty approach during the analysis.
2. Determining the current status of IGA shells in a large-scale application in terms of simulation robustness, stability, simple “plug-and-play” of IGA components, and computational costs.

4.2.2 Side Pole Impact

In a second test case, the isogeometric BIW model is integrated into a side crash model which impacts a rigid pole with 32km/h and at an angle of 75° as shown in Fig. 11 (right) and again compared to a standard FE vehicle model. For the investigations of this load case the focus was on:

1. Studying the robustness and stability of IGA shells in a full vehicle crash scenario with large local deformations (caused by the pole impact) and the corresponding overall behavior.
2. The structural behavior of the seat cross-member as part of the main load path in this side pole impact scenario. In contrast to the longitudinal beam in the front crash, this seat cross-member can be realized as a single-patch IGA model.



*1 Pictures don't show the actual hybrid car model because of confidentiality reasons

Fig.11: Full Width Frontal Impact Setup (left) and Side Pole Impact Setup (right) with components realized as IGA shells highlighted in green.

4.3 Structural Behavior: Full Width Frontal Impact

At first glance the comparison between the FE and the hybrid IGA model showed good agreement. On closer inspection, unexpected element deletion was found in the IGA multi-patch models of the longitudinal beams along patch-coupling edges, which had a significant effect on the deformation of the components. The reason for this element deletion turned out to be an interference of penalty-based patch coupling and conventional edge contact acting on the interpolation shell mesh. As a remedy, a check was implemented in LS-DYNA that automatically excludes interpolation nodes at patch coupling edges from edge contact. Together with improvements on the accuracy of patch boundaries in LS-DYNA, spurious element deletion could be alleviated, leading to comparable behavior between the FE and the hybrid IGA model in terms of global deformation, B-pillar x-acceleration and x-force measured at the rigid wall as shown in Fig. 12. A deformation comparison between the FEA and the IGA longitudinal beam is provided in Fig. 13. As can be seen from Fig. 14, for IGA still a higher number of failed elements is observed, which requires further investigations.

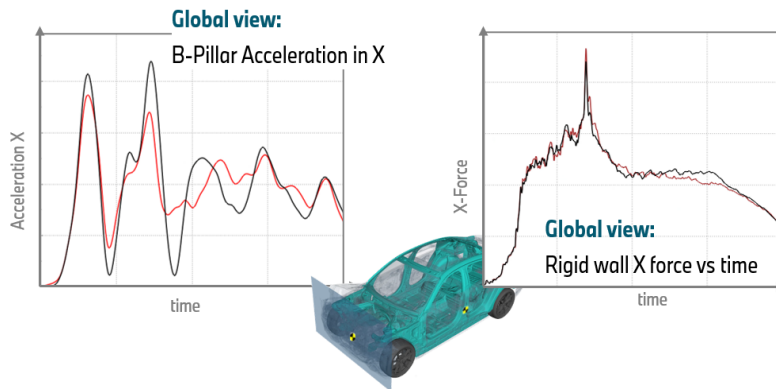


Fig. 12: Global comparison of the IGA simulation (red) and the FEA simulation (black).

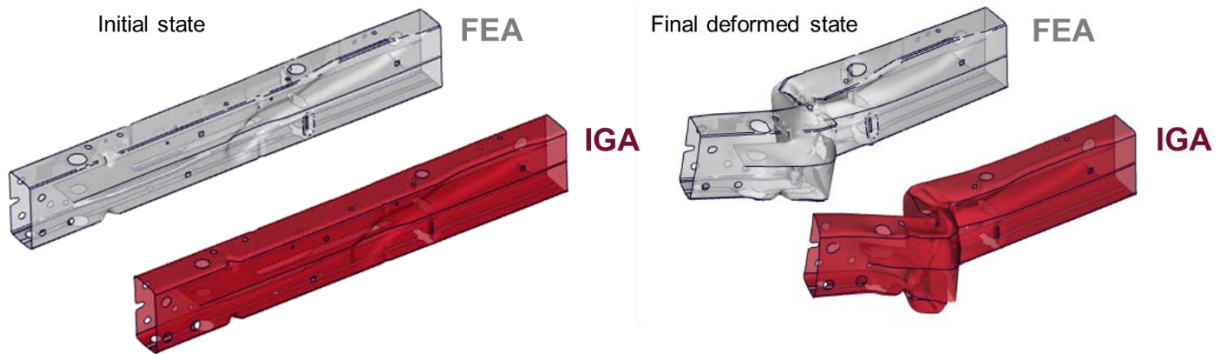


Fig. 13: Deformation of the longitudinal beam in the front crash: Comparison between FEA and IGA.

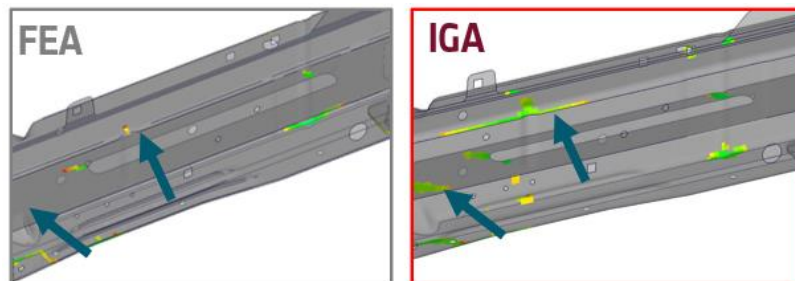


Fig. 14: More deleted elements are observed in certain areas of the IGA model.

4.4 Structural Behavior: Side Pole Impact

Analogous to the front crash scenario, the overall behavior of the hybrid IGA/FEA model shows good agreement with the FE model. A comparison of the global B-pillar displacements and the y-force measured at the pole is provided in Fig. 15.

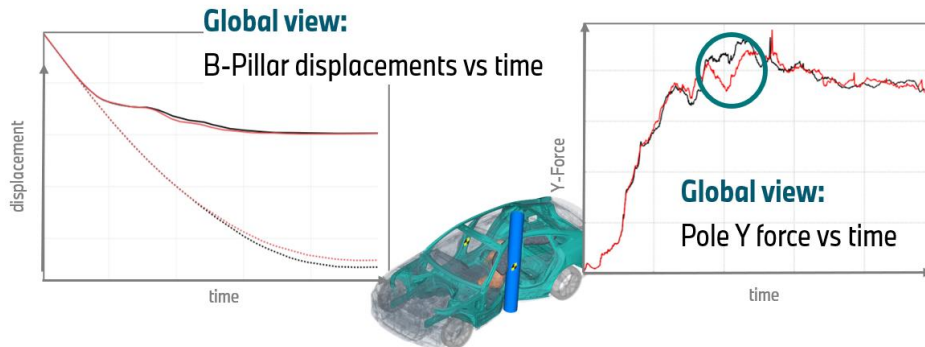


Fig. 15: Global comparison of the B-pillar displacement (left) and the pole force response (right) between the hybrid IGA model (red) and the FE model (black).

While the measured B-pillar displacements show no noticeable differences, one can observe an area of pole force measured in the hybrid IGA model as indicated by a circle. Upon further inspection the seat cross-member is found to have the strong deformations, which is plausible as it lies on the main load path. The differences in the force response may thus be explained by a different buckling and deformation behavior of the seat cross-member, which is strongly determined by the fold trigger holes as shown in Fig. 16.



Fig. 16: Seat cross-member: Comparison of the deformation behavior governed by trigger holes.

Because of that, the different deformation of the IGA and the FEA seat cross-member was expected to be caused by differently modeled trigger holes. Using an IGA approach based on trimmed NURBS patches allows for an accurate geometric description of these holes compared to a relatively rough approximation with linear finite elements. However, the higher-order and higher-continuity NURBS basis functions are also prone to span across small, trimmed cut-outs (small compared to the element size), leading to a local stiffening effect referred to as “Cross-Talk” (a detailed explanation can be found in the conference paper by Lian et al. [5]). Consequently, the question was if this cross-talk effect expected at the trigger holes of the IGA model, could be the reason for the different buckling behavior.

Unfortunately, a serious comparison with hardware tests was not possible at the time of this study, as also mentioned at the beginning of Section 4. Therefore, a very fine IGA seat cross-member model with an average element size of 1mm was created and inserted into the side crash model. This fine IGA model should not suffer from the suspected local stiffening.

A comparison of the seat cross-member deformation modes and force responses for the 4mm FEA model (gray), the 4mm IGA model (red) and the 1mm IGA model (orange) are provided in Fig. 17. As can be seen, the behavior and force response of the 1mm IGA model is very close to the one of the 4mm IGA model. Thus, the IGA results are consistent, indicating that the expected cross-talk effect around the trigger holes in the 4mm IGA model has no significant effect on the buckling mode. Nevertheless, this cross-talk effect and its impact on the model behavior is further investigated on coupon and component level, and research on possible remedies is ongoing [5]. Until then, the deformation behavior of IGA components should be carefully analyzed in areas with potential cross-talk.

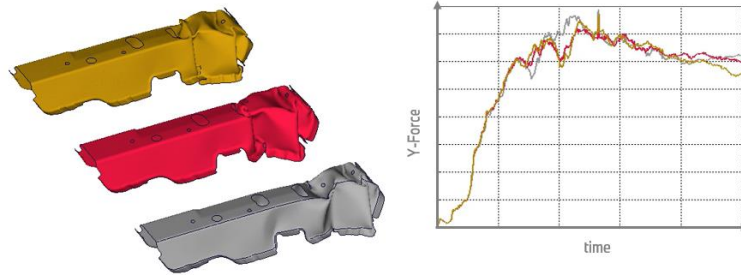


Fig.17: Seat cross-member: Comparison of deformation behavior and force response for the 4mm FEA model (gray), the 4mm IGA model (red) and the 1mm IGA model (orange).

4.5 Computational Costs

For future large-scale IGA adoption, whether to avoid inefficient CAD2CAE processes, to achieve accurate geometric representations, or to profit from future IGA capabilities like feature-based modeling, one major factor is the simulation time. The adoption of IGA into current simulation processes will only occur if doing so does not drastically increase the response time of simulating different model variants.

To get an overview, the simulation times between the conventional FE and the hybrid model simulations are compared. All simulations are performed on the same HPC cluster using 192 CPUs. Analyzing the outputs from the d3hsp files it can be observed that the overall simulation time of the hybrid models is almost twice as high as the one of the FE models. This increase can be broken down into an approximately two times higher overall element processing effort and 1.5 resp. 2 times higher contact processing effort for the front resp. side crash scenario (the side crash scenarios require slightly more contact calculations). This cost overhead for the hybrid model with the current settings is not an unexpected result, given the state of IGA and the experience from previous investigations.

The following remarks shall allow a better interpretation and categorization of the results:

- In the front crash model, the BIW components make up 30% of the total number of elements in the model.
- For both models, the predefined time step of the FE model is used. Thus, the benefit of a larger critical time step for IGA shell elements is not exploited here.
- As a conservative starting point for this investigation, a relatively small average element size of 4mm is chosen for the IGA components, which is similar to the element size of the reference FE model. This is done to allow an accuracy comparison based on a similar mesh size and to ensure high geometric quality. However, as previous studies indicate [2], also using larger element sizes may be appropriate, which would reduce simulation time of the hybrid model. This is subject to current investigations.
- For bi-quadratic IGA shells, one element has $(p + 1) \times (p + 1) = 9$ control points, whereas an FE element shell consists of only 4 nodes. This results in a higher number of function evaluations per integration point. As described in Section 4.1, the bi-quadratic IGA shell elements have a four times higher number of integration points than the FE shell elements with one integration point. This shows that the linear FE shell element is cheaper than the IGA shell element.
- The linear interpolation mesh used for contact of the IGA model is finer than the corresponding FE mesh. With the default settings (NISR=NISS= $p=2$), 2x2 interpolation elements are created for every IGA element. This equates to roughly four times the number of contact segments. A mesh density comparable to the FE model would reduce computational time. This is also subject of current investigations.

5 Conclusion and Outlook

This study demonstrated the creation of an isogeometric BIW model with 288 IGA shell components from CAD data using ANSA. These IGA components were integrated into an existing FE vehicle model, resulting in a hybrid IGA/FEA vehicle model. Full width frontal impact and side pole impact crash simulations were performed in LS-DYNA and subsequently compared to conventional FE simulations in terms of structural behavior and computational costs. In the following, conclusions and proposals for future developments are provided based on the status of IGA in ANSA and LS-DYNA.

5.1 IGA Model Generation Process

The considered BIW consisted mainly of sheet metal components, most of which could be converted automatically, through one click or a batch process, into a single-patch IGA model (257 IGA components of level 1 complexity). For very large sheet metal components like the side panel or extrusion parts like the longitudinal beam, significant manual effort was required for model generation (22 components of level 2 complexity, 9 components of level 3 complexity). For such components, automated IGA surface generation methods still need to be developed to reach the degree of automation of the highly sophisticated FE batch mesh processes at BMW; in fact, the FE shell meshing process for the BIW is almost fully automated [11]. Nevertheless, the already available, automatic IGA surface creation in ANSA provides a simple out-of-the-box solution for a vast majority of sheet metal components, much easier to use than comparable meshing solutions for conventional FEA. Because a midsurface description is also required as a starting point for IGA shell models, the achievable degree of automation also depends on the CAD data quality and the capabilities of midsurface creation tools.

The step after IGA surface creation was the integration of IGA components into an existing FE model. This step was as easy as replacing an FE component and required no or only minor model modifications (node-based connections). This was enabled by implementations in LS-DYNA that allowed using existing connection technology with IGA shells.

Additional advantages of IGA shells regarding the transition speed between CAD and analysis are seen in the feature-based, mesh-independent modeling (e.g. joining technology, boundary conditions, mapping data, multi-material components) analogous to CAD, a consistent data structure for CAD and analysis, and the direct model output from and retransition to the CAD system. Developments in these areas are ongoing or already applicable on a prototypical level.

5.2 Computational Costs

The IGA and FEA shell components considered in this study featured a similar average element size of approximately 4mm. For IGA, bi-quadratic Reissner-Mindling shell elements with reduced Gauss integration are used, for FEA, linear Belytschko-Tsay elements with one integration point. For contact with IGA shells, an interpolation mesh with a density of 2x2 interpolation elements per isogeometric element was used. With these settings, the simulation time for the hybrid IGA vehicle model was observed to be around twice the simulation time of the FEA model in front and side crash scenarios. This outcome is plausible, given that the IGA shell elements used here have a higher number of control points (nodes) and integration points and given the finer contact mesh for IGA. For a large-scale application of IGA in crash simulations, computing time needs to be comparable to FEA simulations. This can be achieved primarily with a larger element size, which seems realistic according to our previous studies and literature. In the long run it will be necessary to find a balance between the predictive quality and simulation time.

Apart from possible code improvements in the future, the following measures are currently investigated to bring IGA simulation times in line with current FEA simulations:

- Use a coarser interpolation mesh size and study the effect on the computational time for contact. The number of interpolation elements per IGA element can be changed using the NISR/NISS options in the `*IGA_SHELL` keyword. Using NISR/NISS=1 instead of =2 results in an interpolation mesh size similar to the FE mesh size.
- Use a larger element size for IGA shell models, either through an automatic coarsening in ANSA (edit functionality) or by generating IGA shell models with larger element size from CAD data. In a first step shell models with 6mm and later with 8mm element size are studied. In regions without strong deformations, even larger element sizes are conceivable.
- Exploit efficiency benefits by using uniform knot vector patches, explicitly defined through UNIR=UNIS=1 in the `*IGA_2D_NURBS_XYZ` keyword.

Finally, it should be noted that the cost overhead observed with these settings does not prevent the application of IGA to specific focus components in the vehicle where the high predictive accuracy of IGA is desired.

5.3 Prediction Quality

In summary, good agreement in the global behavior between the hybrid IGA/FEA and the reference FEA model was observed for both front and side crash scenarios. Because of the larger critical time step of IGA shell elements, a significantly lower amount of mass scaling was necessary for the hybrid model.

On a more detailed level, differences in local deformation patterns of certain components were seen. The question that arises is whether the FEA or the IGA model provides a better representation of the reality. For a better understanding of these local effects, further investigations and research regarding element erosion along the coupling edges of trimmed NURBS patches and the practical influence and minimization of Cross-Talk effects are ongoing.

However, without a comparison to hardware tests, the interpretation of results is difficult. Enabling such comparisons through extended IGA capabilities is therefore the next crucial step. This includes (i) the initialization of IGA shell components with mapped history variables from preceding forming simulations, (ii) improved modeling capabilities for multi-material and multi-thickness components (for tailor-rolled or tailor-welded blanks) for example through multi-PID patches, (iii) validation of the damage evolution behavior for IGA, and (iv) detailed validation of the connection technologies for IGA, especially spotwelds modeled via `*CONSTRAINED_INTERPOLATION_SPOTWELDS`. As demonstrated in the contribution by Leidinger et al. [9], these technologies are currently under development or already available on a prototypical basis. Initialization with mapping data and multi-PID patches, for example, are already available in LS-DYNA, but user-friendly preprocessing workflows are still under development.

5.4 Final remarks

The study has shown that the current IGA capabilities for thin-walled structures in LS-DYNA allow a simple hybrid IGA/FEA model setup with only a few minor adjustments necessary. Furthermore, it has been demonstrated that a large amount of sheet metal parts can be successfully replaced with IGA shells in full hybrid vehicle models and that the models run stably on large clusters. This is a major, necessary step forward for the industrial use of IGA. The higher computational cost in this study was as expected and was explained in detail throughout this paper. Numerous possibilities to reduce the computational cost have been mentioned and will be explored in detail in further studies.

6 Literature

- [1] Hughes, T.J.R., Cottrell, J.A., Bazilevs, Y.: "Isogeometric Analysis: CAD, finite elements, NURBS, exact geometry, and mesh refinement", Computer Methods in Applied Mechanics and Engineering, Vol. 194, 2005, 4135-4195.
- [2] Leidinger, L., Hartmann, S., Benson, D., Nagy, A., Rorris, L., Chalkidis, I., Bauer, F.: "Hybrid IGA/FEA Vehicle Crash Simulations with Trimmed NURBS-based Shells in LS-DYNA", 13th European LS-DYNA Conference 2021, Ulm, Germany.
- [3] Hartmann, S., Leidinger, L., Bauer, F., Benson, D., Nagy, A., Li, L., Pigazzini, M., Nguyen, L.: "Trimmed IGA B-Spline Solids vs. Standard Tetrahedra Finite Elements", 14th European LS-DYNA Conference 2023, Baden-Baden, Germany.
- [4] J.A. Cottrell, T.J.R. Hughes, A. Reali, Studies of refinement and continuity in isogeometric structural analysis, Comput. Methods Appl. Mech. Eng. 196 (2007) 4160–4183.
- [5] Lian, Z., Leidinger, L., Hartmann, S., Bauer, F., Wüchner, R.: "Towards the Solution of Cross-Talk in Explicit Isogeometric B-Rep Analysis", 14th European LS-DYNA Conference 2023, Baden-Baden, Germany.
- [6] Hollweck, C., Leidinger, L., Hartmann, S., Li, L., Wagner, M., Wüchner, R.: "Systematic assessment of isogeometric sheet metal forming simulations based on trimmed, multi-patch NURBS models in LS-DYNA", 14th European LS-DYNA Conference 2023, Baden-Baden, Germany.
- [7] Leidinger, L., "Explicit Isogeometric B-Rep Analysis for Nonlinear Dynamic Crash Simulations", PhD Thesis, Technical University of Munich, Germany, 2020.
- [8] Envyo, <https://www.dynamore.de/en/products/process-chain/envyo>, 2023.
- [9] Leidinger, L., Hartmann, S., Bauer, F., Benson, D., Nagy, A., Li, L., Pigazzini, M., Nguyen, L.: "Enabling Productive Use of Isogeometric Shells in LS-DYNA", 14th European LS-DYNA Conference 2023, Baden-Baden, Germany.
- [10] Leidinger, L., Hartmann, S., Benson, D., Nagy, A., Li, L., Pigazzini, M., Nguyen, L., Bauer, F.: "Isogeometric Shell Components in Full Vehicle Crash Simulations: Hybrid Modeling", 16th LS-DYNA Forum 2022, Bamberg, Germany.
- [11] Näser, B., Tryfonidis, M.: "Development processes with seamless CAD integration in ANSA and DCM", 9th Before Reality Conference 2023, Munich, Germany.